An experimental study of the turbulent mixing layer in concentrated fiber suspensions

Julia Claesson, Tomas Wikström, and Anders Rasmuson

KEYWORDS: Fiber suspension, Turbulence, Mixing layer, LDA

SUMMARY: Turbulence structures in a free mixing layer after a backward-facing step were studied in concentrated pulp suspensions (0.5-3% by weight) using Laser Doppler Anemometry (LDA) at two predetermined average inflow velocities (0.9 and 1.8 m/s). Both average and fluctuating velocities were investigated and the findings were compared with measurements in water. The experimental findings show that both the average velocities and the RMS velocities in the mixing layer decreased with an increase in concentration. Furthermore, by analyzing the energy spectra at the center of the mixing layer, it was possible to extract the inertial sub-range of pulp suspensions with a concentration of 0.5% at the lower inflow velocity and in suspensions up to a concentration of 1% at the higher inflow velocity. At higher concentrations the turbulence was damped by the fiber network and no turbulence structures could be extracted. The energy content at lower frequencies was higher in the pulp suspensions than in the experiments in pure water.

ADDRESSES OF THE AUTHORS: Julia Claesson (julia.claesson@chalmers.se) and **Anders Rasmuson** (rasmuson@chalmers.se): Chalmers University of Technology, Department of Chemical and Biological Engineering, SE-412 96 Gothenburg, Sweden. **Tomas Wikström** (tomas.vikstrom@metso.com): Metso Paper Sundsvall AB, SE-851 94 Sundsvall, Sweden
Corresponding author: Anders Rasmuson

In several types of process equipment in engineering applications free mixing layers are found, e.g., in mixing vessels, heat exchangers and reactors. The flow structures in Newtonian turbulent free mixing layers after a sudden expansion have been studied by several research groups. Mathematical models of boundary layers and jet flows in Newtonian flows have been derived by Schlichting (2003) and Rajaratnam (1976). Experimental studies of the flow in Newtonian flows after a sudden expansion have, e.g., been studied using Ultrasound Velocity Profiling technique (UVP) by Inoue at al. (2002) and Furuichi et al. (2003). In the study by Inoue et al. (2002) the frequency spectra in the free turbulent mixing layer in a three-dimensional jet from a square nozzle were studied, and Furuichi et al. (2003) studied the fluctuations of the reattachment point after a sudden expansion at varied flow rates. In both studies the velocity fluctuations were analyzed with wavelet transforms and proper orthogonal decomposition, with those techniques flow structures with frequencies containing most of the energy was possible to analyze in more detail.

Experimental studies of turbulent jets in solid-liquid and solid-gas flows in concentrations up to 6.2% have been performed by Virdung and Rasmuson (2007), Fan et al. (1992), Sheen et al. (1994) and Eng (2012). In these studies the solid fraction consisted of spherical particles that were free to follow the flow. Fan et al. (1992) and Sheen et al. (1994) have shown that the spreading rate and the centerline velocity decreased when particles were added to a gas flow in contrast to Eng (2012) who did not observed any changes in the width or centerline velocity when particles were added to a liquid flow. Virdung and Rasmuson (2007) and Eng (2012) have shown, however, that the RMS velocities increased with an increase in concentration.

In contrast to particle-liquid flow, where particles are free to follow the flow, the fibers in a fiber-liquid flow are connected to each other at concentrations even below 1% depending on the fiber dimensions. (Kerekes 2006). The fibers form flocs and coherent networks which are disrupted when the energy in the flow increases. When a fully turbulent flow is reached the fiber network is totally broken (Fock et al. 2011). In the laminar regime, the fiber network increases the viscous forces in the flow similar to a single-phase flow, however, two-phase effects continue to affect the flow structures (Wikström, Rasmuson 1998).

Experimental studies of the flow of pulp suspensions after a sudden expansion have been conducted by several researchers (Arola et al. 1998; Heath et al. 2007; Karema et al. 1999; Claesson et al. 2012a; 2012b). In addition to these studies Andersson and Rasmuson (2000), Ljus et al. (2002) and Steen (1989) have studied turbulent structures in fiber-liquid and fiber-gas flows. Andersson and Rasmuson (2000) have studied the transition point and turbulent structures in glass fiber suspensions with a concentration of 3-20% in a mixer using Laser Doppler Anemometry (LDA). Findings show that it was possible to extract turbulence information from concentrated refractive index-matched glass fiber suspensions using LDA. In the study by Ljus et al (2002) both fiber-gas and particle-gas flows were studied using a hot wire. The fiber-gas flow was studied at a concentration of 0.01 and 0.03%. At the lower concentration no effect on the average velocity profile or the turbulence structures was observed. However, at the higher concentration a significant effect on the flow field and turbulence was observed. When the turbulent spectra were analyzed it was concluded that the turbulent energy decreased at all frequencies above 9 Hz, however, below 9 Hz there was a significant increase in turbulent energy. Steen (1989) used LDA to study the turbulent structures in glass fiber refractive index-matched suspensions at two different fiber lengths; 1 and 3 mm, at concentrations of 0.12 and 1.2%. It was found that the turbulent energy was higher at the smaller length scales at the lower concentration with 1 mm fibers due to the rotation of free fibers. In suspensions with fibers with a length of 3 mm and a

concentration of 1.2%, a decrease in turbulent energy was observed at all length scales.

There is a vital lack of detailed turbulence studies in concentrated fiber suspensions. The aim of the present study was thus to investigate turbulence and turbulent structures produced in a free mixing layer. For that purpose equipment was developed where the free mixing layer, formed after a backward-facing step in concentrated fiber suspensions (0-3% by weight), could be studied at different average inflow velocities. The experimental technique used was Laser Doppler Anemometry (LDA).

Experimental method and set-up

Laser Doppler Anemometry

Laser Doppler Anemometry (LDA) is an optical velocity measurement technique for transparent liquids and gases seeded with seed particles. When velocities are measured, the reflecting light from the seed particles that flow though the cross section of two laser beams at the same, but phase-shifted, frequency, forming a well-defined interference pattern, are collected and recalculated to velocities in a Burst Spectrum Analyzer (BSA). LDA is a continuous measurement technique that collects all valid bursts at each measurement position during a pre-defined measurement time or the time needed to collect a pre-defined number of valid bursts. As a consequence, the data collected is unevenly distributed in time (Durst et al. 1981).

Pulp suspensions are opaque liquids at fiber concentrations down to at least 0.5% by weight. This factor complicates making velocity measurements employing optical measurement techniques. However, studies have shown that it is possible to measure velocities several millimeters into pulp suspensions with concentrations up to at least 7.8% (Kerekes, Garner, 1982; Pettersson, Rasmuson, 2004; Wiklund et al. 2006; Pettersson et al., 2006; Claesson et al, 2012b). Measurements using LDA are possible to perform at these concentrations since laser light is able to penetrate a suspension by passing between fibers.

In the experiments 1D measurements were performed using a DANTEC FiberFlow Series 60X (Skovlunde, Denmark) LDA connected to a DANTEC 57N10 BSA controlled by DANTEC's BSA Flow software. A Spectra-Physics laser (Model 2060A-64, Dramstadt, Germany) was used. The laser probe was fixed on a traverse that was movable in the x, y and z directions. In all cases, except in the experiments in pure water, fibers were used as the seed particles. For the experiments in water, the seed particles used were S-HGS silver-coated hollow glass spheres with a density of 1.3 kg/dm^3 and a diameter of 10 μm.

Experimental set-up

A flow loop designed by Pettersson et al. (2006) was used in the experimental study. The flow loop consisted of a 300 l open tank placed on a progressive cavity pump with a maximum flow rate of 180 l/min. The pump was connected to a stainless steel pipe with a diameter of 100 mm which was used to circulate the fluid back to the open tank. A customized test section with a cross section of 40x40 mm^2 was placed close in front of the tank. This was where the free mixing layer was studied. The stainless steel pipe was connected to the test section via a contraction unit which decreased the diameter from 100 mm to 40 mm. More details concerning the flow loop can be found in Pettersson et al. (2006). The customized test section used was a squared pipe with a cross section of 40x40 mm^2 and a length of 380 mm made of 5 mm thick Plexiglas.

To be able to create and study turbulence a block with a height of 30 mm was placed at the entrance of the test section, over which the free mixing layer was formed. To minimize the formation of a secondary flow with a stagnation point in front of the block at higher concentrations the block was beveled. A schematic picture of the test section is shown in *Fig 1*.

Material and Experimental procedure

Fully bleached never-dried softwood kraft pulp at a concentration of about 20% provided by Södra Cell Värö was used in the study. The length and diameter of the fibers were measured with a Kajaani FS300 made by Metso. The average length of the fibers was approximately 2 mm and the average diameter was approximately 25 μm. In the study experiments were performed in pulp suspensions at a concentration of 0, 0.5, 1, 2 and 3% by weight at an average inflow velocity of 0.9 and 1.8 m/s at x=0 cm (see *Fig 1*), corresponding to a Reynolds number of 9 000 and 18 000 in water. Velocity data was collected along the y-axis from y=39 mm to y=1 mm, in steps of 1 mm, at x=10, 20 and 50 mm according to *Fig 1*. All measurements except the experiments in pure water were performed at 2.5 mm from the wall perpendicular to the flow. Measurements close to the wall were performed to increase the data rate. If the distance was increased further the fibers blocked the laser beams and the data rate dropped.

Findings from the study of the near wall boundary layer in concentrated pulp suspensions by Pettersson et al. (2006) show that the plug flow is reached at 0.2 mm from the wall at the same concentrations and velocities as in this study. This implies that the main flow could be measured at 2.5 mm from the wall. However, the measurements in clear water were performed at the center of the pipe, i.e., at 20 mm from the wall, due to the low data rate closer to the wall. In all measurement positions maximum 20 000 valid bursts were collected during 30 seconds. Depending on the concentration and velocity the frequency varied between the different cases. At greater concentration the frequency increased, probably because there was greater potential for a fiber to flow through the measurement volume. The frequency in the collected data varied from 100 to 8000 Hz.

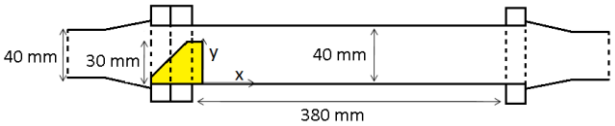

Fig 1. A schematic picture of the test section

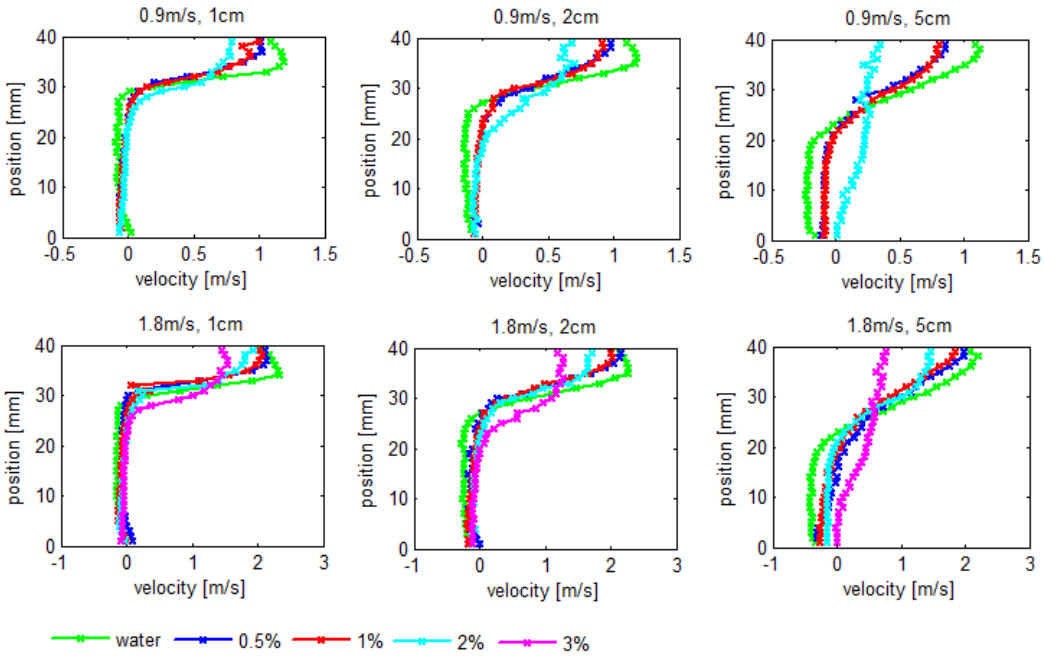

Fig 2. The average measured velocity profiles at all measurement positions along the x-axis

Data analysis

Analyses of the collected data were performed in Matlab. At all measurement positions both the average velocity and the root mean square (RMS) velocity were calculated. The RMS velocity was calculated by using *Eq 1*, where u_i are the measured velocities, U_{avg} is the average velocity and N is the number of valid bursts collected.

$$u' = \sqrt{\frac{\sum_{i=1}^{N}(u_i - U_{avg})^2}{N}} \qquad [1]$$

To investigate turbulence, the frequency in the data was analyzed using the Lomb algorithm. The Lomb algorithm has the potential to investigate frequencies in unevenly spaced data in time in contrast to a normal Fast Fourier Transform (FFT) (Lomb 1975).

Results and discussion

Velocity profiles

The average velocity profile measured along the y-axis at each position in the x direction, except the measurements done at an average inflow velocity of 0.9 m/s and 3%, are shown in *Fig 2*. The measurements at 0.9 m/s and 3% were excluded since the flow was drastically reduced at x=0 cm by the almost stagnant zone in the test section, therefore no mixing layer was formed at those flow conditions. *Fig 2* shows that the mixing layer between the main flow and the recirculation flow is found at approximately y=30 mm at x=1 cm, which is the step height. The position of the mixing layer decreases to approximately y=20 mm at x=5 cm. Another observation made was that the length of the mixing layer, i.e., the reattachment length decreased with an increase in concentration or a decrease in velocity in accordance with Claesson et al. (2012b). As can be seen in *Fig 2*, the reattachment point was reached at approximately x=5 cm in the suspensions with a concentration of 2% at an inflow velocity of 0.9 m/s, and in the suspension with a concentration of 3% at an inflow velocity of 1.8 m/s. Further details regarding the reattachment length were not investigated in this study. In *Table 1* the maximum average velocities and the maximum average recirculation velocities measured are presented. According to *Fig 2* and *Table 1* both the velocity and the recirculation velocity decreased when the concentration increased. This was also observed by Claesson et al. (2012b). The maximum velocity was rather stable along the x-axis in suspensions with concentrations from 0 to 1%. At 2 and 3% the maximum velocity dropped along the x-axis due to the reduced reattachment length. When the recirculation velocity was studied at the higher inflow velocity it was observed to increase along the x-axis in all suspensions except the suspension with a concentration of 3%, in contrast to the more stable recirculation velocity at the lower inflow velocity.

RMS profiles

The RMS velocity profile measured along the y-axis at each position in the x direction, except the measurements made at 0.9 m/s and 3%, are shown in *Fig 3*. The peak in the RMS profiles shows where the velocity fluctuations were the largest, which was found in the mixing layer directly above the recirculation zone, see *Figs 2* and *3*. According to *Fig 3* the width of the peak, i.e., the mixing layer, increased along the x-axis. This was also observed by Claesson et al. (2012a). In *Table 2* the maximum RMS velocities and the width of the RMS peak, i.e., the width of the mixing layer are presented for all cases studied. The findings show that the RMS velocities decreased when the concentration was increased in accordance with Claesson et al. (2012b), see *Table 2*. This could be compared with Virdung and Rasmuson (2007) and Eng (2012) who showed that the RMS velocities increased with an increase in particle concentration of spherical particles.

Table 1. The maximum average velocity and the maximum average recirculation flow at all measurement positions along the x-axis

Conc. [%]	0.9 m/s U_{max} [m/s]			1.8 m/s U_{max} [m/s]			0.9 m/s $U_{R,max}$ [m/s]			1.8 m/s $U_{R,max}$ [m/s]		
	1 cm	2 cm	5cm	1 cm	2 cm	5cm	1 cm	2 cm	5cm	1 cm	2 cm	5cm
0	1.19	1.18	1.12	2.34	2.27	2.20	0.09	0.14	0.24	0.16	0.28	0.43
0.5	1.02	0.98	0.86	2.12	2.16	1.98	0.07	0.07	0.11	0.09	0.18	0.31
1	1.00	0.93	0.81	2.06	2.02	1.84	0.07	0.07	0.10	0.13	0.20	0.28
2	0.79	0.70	0.35	1.94	1.72	1.46	0.07	0.08	-	0.10	0.12	0.16
3	-	-	-	1.54	1.28	0.77	-	-	-	0.09	0.12	0.02

Table 2. The maximum RMS velocities and the width of the RMS peak measured at all measurement positions along the x-axis

Conc. [%]	0.9 m/s u'_{max} [m/s]			1.8 m/s u'_{max} [m/s]			0.9 m/s width [m/s]			1.8 m/s width [mm]		
	1 cm	2 cm	5cm	1 cm	2 cm	5cm	1 cm	2 cm	5cm	1 cm	2 cm	5cm
0	0.42	0.45	0.43	0.55	0.58	0.61	10	13	23	10	15	28
0.5	0.30	0.26	0.22	0.65	0.60	0.57	8	11	15	7	11	24
1	0.28	0.22	0.20	0.64	0.63	0.45	8	11	15	6	11	21
2	0.23	0.20	0.12	0.33	0.50	0.35	10	17	-	8	7	13
3	-	-	-	0.37	0.45	0.18	-	-	-	8	7	-

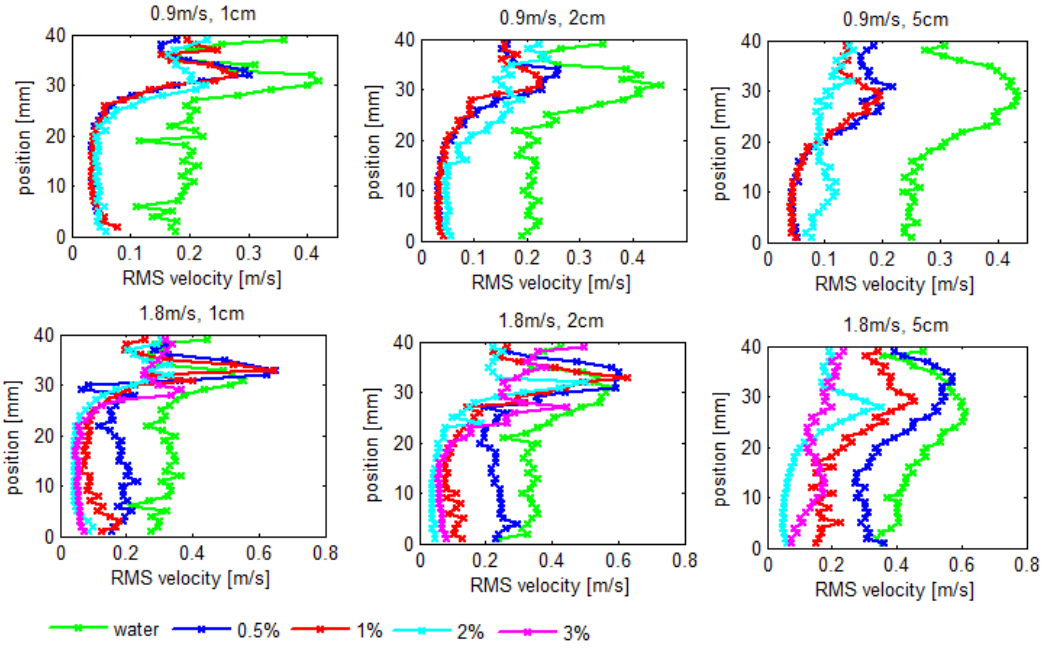

Fig 3. The RMS velocity profiles in all measurement positions along the x-axis.

In contrast to these studies, fiber flows are expected to be more complex due to fiber-fiber interactions and entanglement. The structures and fibers in the network will be larger than the smaller turbulent eddies in the flow, and the fiber network will therefore have a dampening effect on turbulence. At a greater concentration the network becomes even stronger, which results in an increase in the dampening effect of the flow, i.e., decreased RMS velocities. Furthermore, for all experiments, except the measurements in pure water at the lower average inflow velocity, the maximum RMS values measured were approximately 27% of the average inflow velocity at x=0 cm. Another observation made was that the maximum RMS velocity decreased along the x-axis, this was clearer at the lower inflow velocity. According to *Table 2* the width of the mixing layer was wider in water and decreased with greater fiber concentration. As mentioned above, at an increase in concentration the fiber network has a dampening effect on turbulent eddies which results in a thinner mixing layer. Furthermore, at a higher inflow velocity the width increases more along the x-axis than the width at the lower average inflow velocity. This is probably due to the higher energy in the flow which disrupts the fiber network more effectively, especially at lower concentrations where the network is weaker. When the width of the main flow was studied in *Fig 2* it was observed to be similar for all cases except the suspension with a concentration of 2% at an inflow velocity of 0.9 m/s, and the suspension with a concentration of 3% at an inflow velocity of 1.8 m/s. This indicates that the fibers do not affect the main flow but

lower the velocity fluctuations, i.e., the size of the RMS peak, in the first part of the test section

To further investigate the structure in the mixing layer, contour plots of the 500 first collected velocities at an average inflow velocity of 1.8 m/s measured at x=20 mm and y=35-20 mm are shown in Figure 4. According to *Fig 4* the velocity fluctuations in the mixing layer are smoothed when the concentration increases in accordance with *Fig 3*, where the velocity fluctuations decrease with greater concentration. The width of the main flow is rather unaffected by the concentration as can be seen in *Fig 2*. However, the width of the mixing layer, where the interaction between the main flow and the recirculation flow occurs, is wider at lower concentrations. At a concentration of 2% and especially 3% the shorter reattachment length affects the width of the main flow, and further affects the position of the mixing layer as shown in *Figs 2* and *3*. When the contour plots of the mixing layer were studied at the other measurement positions similar trends were observed.

Turbulence spectra

Turbulence energy spectra were determined using the Lomb algorithm. The slope in the resulting energy spectra was compared with the well-known Kolmogorov 5/3 law. The 5/3 law describes the region in the turbulence spectra where the inertial sub-range exists, i.e., the region where no turbulent kinetic energy is produced or dissipated only transported to smaller eddies. If the slope of $E \propto f^{-5/3}$ was possible to extract in the energy spectra, the flow at that measurement position was assumed to be fully turbulent (Tennekes, Lumley 1992). *Fig 5* shows energy spectra from measurement positions in the mixing layer at the lower average inflow velocity. Included in the spectra is the slope at $\propto f^{-5/3}$. The spectra shown are from measurement positions at the step height (y=30 mm), i.e., where the RMS values were the highest, see *Fig 3*. In *Fig 5* the spectra in pure water at x=1 cm were excluded due to the low data rate at those measurement positions. *Fig 6* shows the corresponding energy spectra at the higher average inflow velocity. The spectra measured in the suspension with a concentration of 0.5% are excluded from the figure due to the low data rate. As can be seen in *Figs 5* and *6* the slope of the curve deviated from $E \propto f^{-5/3}$ in some of the spectra. To investigate the impact of the fiber network on the turbulent structures the slope in each of the spectra shown in *Figs 5* and *6* was studied in detail. The findings for these slopes are given in *Table 3*. As can be seen in *Table 3*, the slope in most of the spectra at x=1 cm deviated from $f^{5/3}$. It was noted that an increase in concentration decreased the slope. The slope was more damped probably due to a more laminar flow close to the entrance of the nozzle, in accordance with studies of a free Newtonian jet which has been shown to have a laminar zone close to the nozzle (Tennekes, Lumley 1992). When the concentration increases the fiber network becomes stronger and more energy is needed to disrupt the network. This may result in a more damped slope in the energy spectrum. At x=5 cm the inertial sub-range was found in suspensions with a concentration of 0.5% at the lower inflow velocity, and in a suspension up to a concentration of 1% it was found at the higher inflow velocity. This indicates that the energy in the mixing layer, in those cases, was high enough to disrupt the network and still remain in the turbulent regime. In spectra where the inertial sub-range exists, the inertial sub-range was found in the frequency band from approximately 10 Hz to 100 Hz, which corresponds to a wavelength of 10 and 1 mm.

Table 3. The slope in each of the energy spectra

Conc.	0.9 m/s		1.8 m/s	
[%]	1 cm	5cm	1 cm	5cm
0	-	$f^{-5/3}$	$f^{-5/3}$	$f^{-5/3}$
0.5	$f^{-5/4}$	$f^{-5/3}$	-	-
1	$f^{-5/4}$	$f^{-5/4}$	$f^{-5/4}$	$f^{-5/3}$
2	$f^{-5/6}$	$f^{-5/3}$	f^{-1}	$f^{-5/4}$
3	-	-	f^{-1}	$f^{-5/3}$

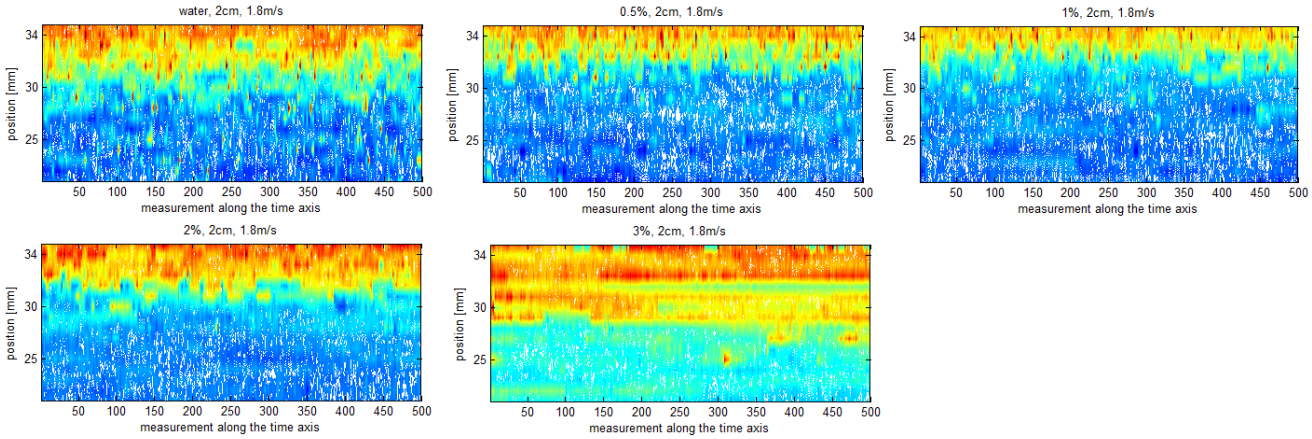

Fig 4. Contour plots of the 500 first collected velocities at x=20mm and y=35-20mm from the measurement position at an average velocity of 1.8m/s at varied concentrations.

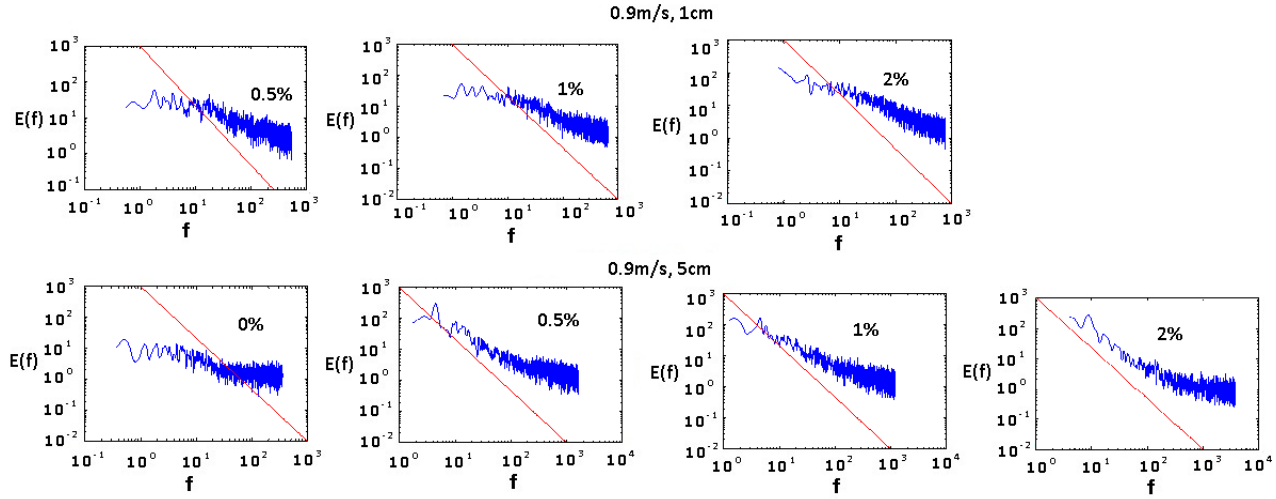

Fig 5. The frequency spectra at the position of the step height for the measurement at an average inflow velocity of 0.9m/s. The figures include $E \propto f^{-5/3}$

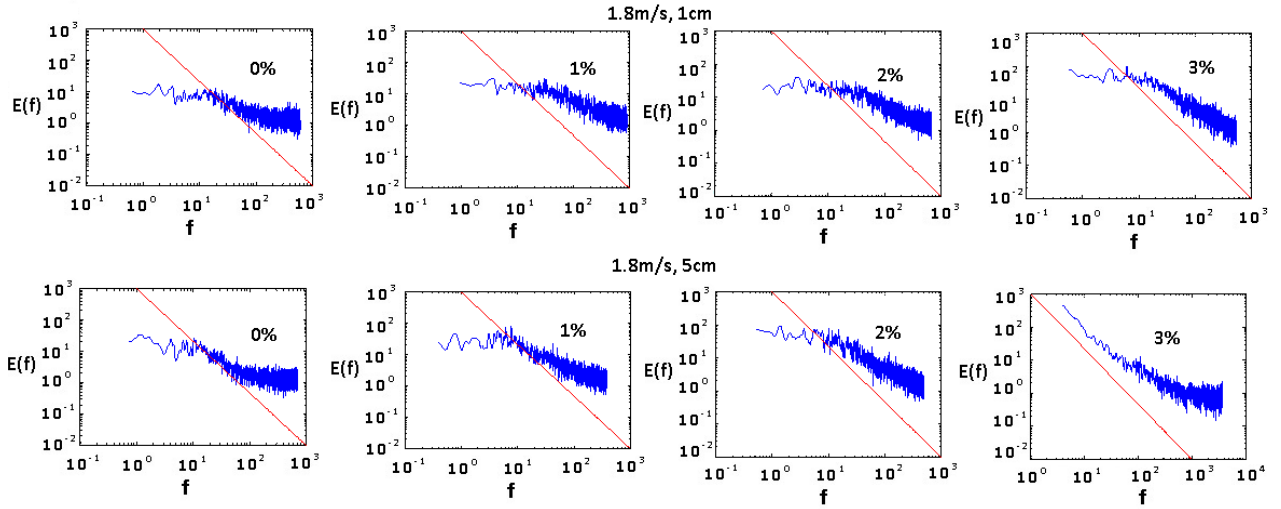

Fig 6. The frequency spectra at the position of the step height for the measurement at an average inflow velocity of 1.8m/s. The figures include $E \propto f^{-5/3}$

The flocs in the pulp suspensions are in the range of 10 mm, and the rotation radius of a fiber is 1 mm. This indicates that turbulent eddies with a wavelength smaller than 1 mm are dissipated. Similar results were found in the recirculation zone in pulp suspensions after a backward-facing step (Claesson et al. 2012a). Furthermore, as mentioned above, the spectra at x=5 cm in the suspension with a concentration of 2% at an inflow velocity of 0.9 m/s and in the suspension with a concentration of 3% at an inflow velocity of 1.8 m/s were from measurement positions above the reattachment point, i.e., at the position where there was no mixing layer. These two spectra show that the flow was turbulent at the position where the main flow was drastically reduced by the more stagnant flow further downstream. Similar findings were observed by Heath and Olson (2007) who obtained a fully fluidized jet in suspensions with a concentration of 0.4% at an upstream velocity of 0.9 m/s.

When the energy level in the spectra at the lower inflow velocity was studied, the energy found at frequencies below 10 Hz in all pulp fiber suspensions at x=5 cm was greater than in clear water, similar to findings by Ljus et al. (2002) (*Fig 5*). An increase in energy at frequencies below 10 Hz was also found at the higher inflow velocity at x=5 cm in the suspension with a concentration of 2 to 3%. The increase in turbulent energy at lower frequencies may be produced in the wake after the flocs. At the lower inflow velocity, the energy in the flow may not be high enough to disrupt flocs in fiber suspensions at a concentration of 0.5%. This can be compared to the experiments with the higher inflow velocity where the energy increase at lower frequencies is found first at a concentration of 2 to 3%.

Conclusions

In the study it was concluded that both the average maximum velocity and the maximum average recirculation velocity decreased when the concentration increased. A higher concentration gave a stronger network which increased the energy content in the fluid. A fluid with a stronger network could therefore be more difficult to accelerate and the maximum velocities could be lower. Furthermore, findings from the experiments

show that the velocity fluctuations decreased with an increase in concentration and decreased along the mixing layer. At all positions at the lower inflow velocity the measured RMS velocity in pure water was approximately 40% higher than the RMS velocities in the concentrated fiber suspensions. However, at the higher inflow velocity the measured RMS velocities were almost the same in the fiber concentration range 0-1%. Moreover, the maximum RMS velocities measured were approximately 27% of the average inflow velocity at x=0 cm.

When the frequencies in the data in the mixing layer at the lower inflow velocity were analyzed the inertial sub-range was found only at x=5 cm in suspensions up to a concentration of 0.5%. At the higher inflow velocity the inertial sub-range was found in a suspension up to a concentration of 1% at x=5 cm. The inertial sub-range was detected in the frequency range 10 to 100 Hz. At x=1 cm the turbulence was damped by the fiber network and the slope $\propto f^{-5/3}$, i.e., the inertial sub-range, was not found. Another observation made was that the energy content at lower frequencies, shown in spectra from measurement positions at x=5 cm, was greater in the fiber suspensions than in clear water. This may be due to the production of turbulence in the wake formed after the flocs that are not disrupted in the flow.

Acknowledgements

This work is part of a PhD project financed by the Swedish Energy Agency.

Literature

Andersson, S.R. and Rasmuson, A. (2000): Flow measurement on a turbulent fiber suspension by laser doppler anemometry, AIChE Journal, 46(6), 1106-1119.

Arola, D.F., McCarthy, M.J., Li, T-Q. and Ödberg, L. (1998): NMR imaging of pulp suspension flowing through an abrupt pipe expansion, AIChE Journal, 44(12), 2597-2606.

Claesson, J., Wikström, T. and Rasmuson, A. (2012a): Measurement and analysis of flow of concentrated fiber suspensions through a 2-D sudden expansion using UVP, AIChE Journal, Early view access.

Claesson, J., Wikström, T. and Rasmuson, A. (2012b): Flow of concentrated fiber suspensions over a backward facing step studied using LDA, Nord. Pulp Paper Res J.,27(3), 653-661.

Durst, F., Melling, A. and Whitelaw, J. (1981): Principles and practice of Laser Doppler Anemometry, Academic Press.

Eng, M. (2012): Flow structures in solid-liquid suspensions in mixing and confined jets, Licentiate thesis, Chalmers university of technology.

Fan, J., Zhao, H. and Can, K. (1992); An experimental-study of 2-phase turbulent coaxial jets, Experiments in Fluids, 13(4), 279-287.

Fock, H., Claesson, J., Wikstrom, T. and Rasmuson, A. (2011): Near wall effects in the plug flow of pulp suspensions, The Canadian Journal of Chemical Engineering, 89(5), 1207-1216.

Furuichi, N., Takeda, M. and Kumada, M. (2003): Spatial structure of the flow through an axisymetric sudden expansion, Experiments in Fluids, 34(5), 643-650.

Heath, S. J. and Olson, J. A. (2007): Visualization of the flow of a fiber suspension through a sudden expansion using PET, AIChE Journal, 53(2), 327-334.

Inoue, Y., Yamashita, S. and Kondo, K. (2002): The ultrasonic profile measurement of flow structures in the near field of a square free jet, Experiments in Fluids, 32(2),170-178.

Karema, H., Kataja, M., Kellomäki, M., Salmela, J. and Selenius, P. (1999): Transient fluidisation of fibre suspension in straight channel flow, TAPPI international paper physics conference, 369-379.

Kerekes, R.J. (2006): Rheology of suspensions - Rheology of fiber suspensions in papermaking: an overview of recent research, Nord. Pulp Paper Res J., 21(5), 598-612.

Kerekes, R.J. and Garner, R.G. (1982): Measurement of turbulence in pulp suspension by laser anememotry. Tans. Tech. Sect. CPPA, 8, TR53-TR60.

Ljus, C., Johansson, B. and Almstedt, A-E. (2002): Turbulence modification by particles in horizontal pipe flow, International Journal of Multiphase Flow, 28(7), 1075-1090.

Lomb, N.R. (1975): Least-square frequency analysis of unequally spaced data, Astrophysics and Space Science,39(2), 447-462.

Pettersson, J. and Rasmuson, A. (2004): LDA measurements on a turbulent gas/liquid/fibre suspension, Canadian Journal of Chemical Engineering, 82(2), 265-274.

Pettersson, A.J., Wikström, T. and Rasmuson, A. (2006): Near wall studies of pulp suspension flow using LDA, Canadian Journal of Chemical Engineering, 84(4), 422-430.

Rajaratnam, N. (1976): Turbulent jets. USA, Elsevier Scientific Pub. Co.

Schlichting, D.H. (2003): Boundary-Layer Theory. Germany, Berlin, Springer.cop.

Sheen, H.J., Jou, B.H. and Lee, Y.T. (1994): Effect of particle-size on a 2-phase turbulent jet. Experimental Thermal and Fluid Science, 8(4), 315-327.

Steen, M. (1989): On turbulence structure in vertical pipe flow of fiber suspensions, Nord. Pulp Paper Res. J., 4(4), 244-252.

Tennekes, H. and Lumley J.L. (1992): A first course in turbulence, 14th printing, The MIT press.

Virdung, T. and Rasmuson, A. (2007): Hydrodynamic properties of a turbulent confined solid-liquid jet evaluated using PIV and CFD., Chemical Engineering Science, 62(21), 5963-5978.

Wiklund, J.A., Stading, M., Pettersson, A.J. and Rasmuson, A. (2006): A comparative study of UVP and LDA techniques for pulp suspensions in pipe flow, AIChE Journal, 52(2), 484-459.

Wikström, T. and Rasmuson, A. (1998): The agitation of pulp suspensions with a jet nozzle agitator, Nord. Pulp Paper Res. J., 13(2), 88-94.

Manuscript received June 12, 2012

Accepted October 30, 2012